Electronic Supplementary Material (ESI) for Materials Advances.

SUPPLEMENTARY INFORMATION

Organic Cation (DMPI) Intercalated Graphite Anode for High Voltage Next Generation Dual-Ion Battery

Surya Sekhar Manna, † Sandeep Das, † Arunendu Das, † Biswarup Pathak, †, *

† Department of Chemistry Indian Institute of Technology (IIT) Indore, Indore, Madhya Pradesh 453552, India
*Email: biswarup@iiti.ac.in

Contents:

Figure S6. Pictorial representation of $6 \times 6 \times 2$ supercell of stage-2 DMPI intercalated graphite system with different DMPI cation concentration, (a) $C_{288}(DMPI)_2$, (b) $C_{288}(DMPI)_4$, (c) $C_{288}(DMPI)_6$ and (d) $C_{288}(DMPI)_8$.

Figure S7. Pictorial representation of $6 \times 6 \times 3$ supercell of stage-3 DMPI intercalated graphite system with different DMPI cation concentration, (a) $C_{432}(DMPI)_2$, (b) $C_{432}(DMPI)_4$, (c) $C_{432}(DMPI)_6$ and (d) $C_{432}(DMPI)_8$.

Figure S8. Pictorial representation of $6 \times 6 \times 2$ supercell of stage-4 DMPI intercalated graphite system with different DMPI cation concentration, (a) $C_{288}(DMPI)_1$, (b) $C_{288}(DMPI)_2$, (c) $C_{288}(DMPI)_3$ and (d) $C_{288}(DMPI)_4$.

Figure S9. Schematic representation of NBO charge analysis on the C2 carbon atom of (a) DMPI and (b) EMI cations.

Figure S10. Simulated XRD pattern of the different staging of DMPI intercalated graphite system and pristine graphite where 2θ ranges in 3° – 65°.

Figure S11. Systematic illustration of different staging mechanism of $AlCl_4$ anion intercalation, (a) graphite, (b) stage-4, (c) stage-2, and (d) stage-1, where R.E (eV) is the relative energies of same concentration of $AlCl_4$ ions. Here, brown, blue and green colour represents carbon, aluminium and chlorin, respectively.

Figure S12. Schematic representation of the four diffusion barriers pathway, where (a-d) corresponds to path 1-4.

Table S1. Relative energy (eV) of the different binding sites of the DMPI cation intercalated graphite system.

Sites	Relative Energy (eV)
Top	0.009
Hollow	0.000
Bridge-1	0.045
Bridge-2	0.038

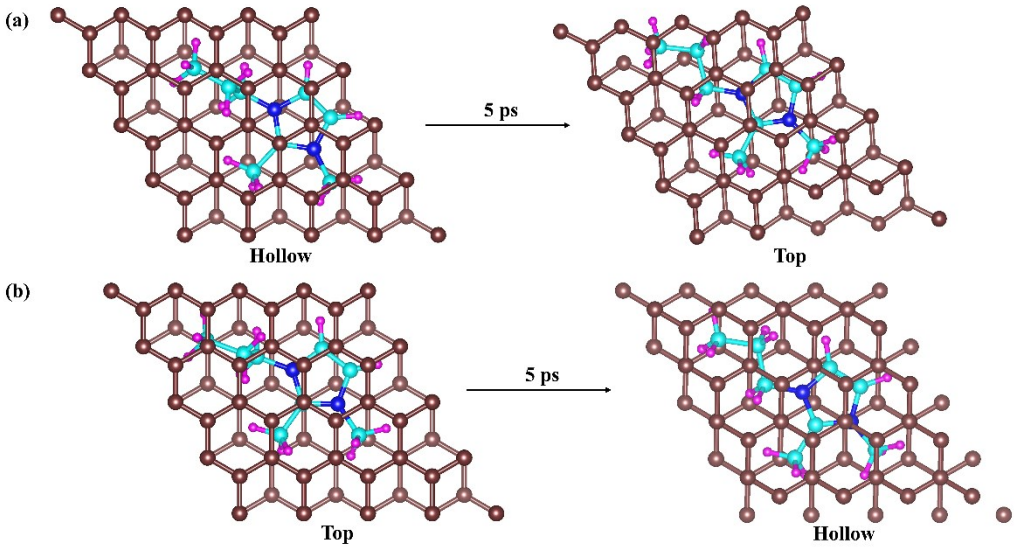

Figure S1. Schematic representation of changing adsorption sites between Hollow and Top sites of the DMPI cation inside the graphite anode through the molecular dynamics simulation at 300 K temperature, (a) Hollow to Top and (b) Top to Hollow.

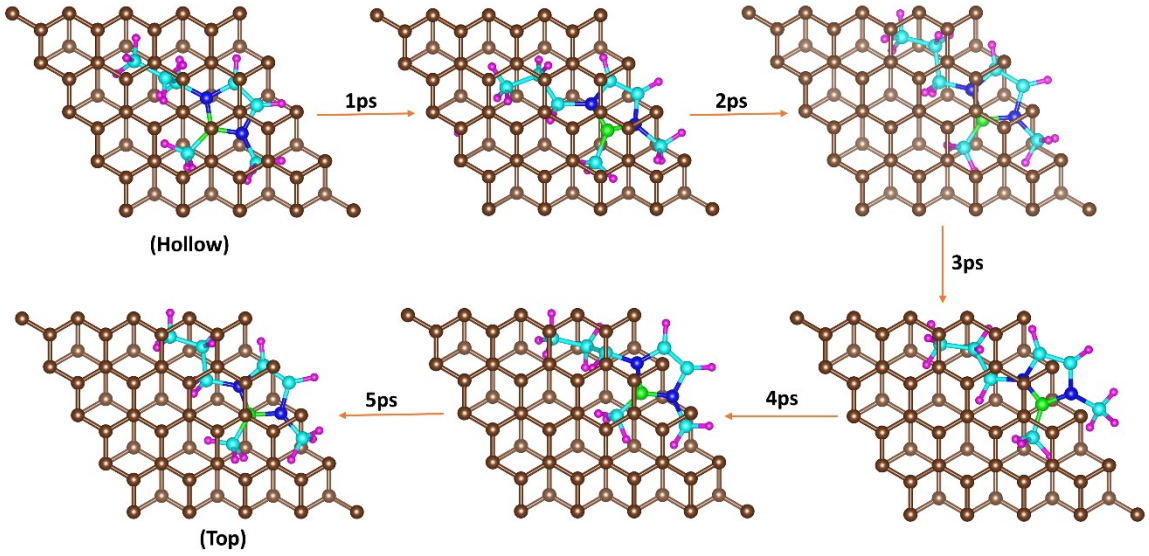

Figure S2. The interconversion step of most stable site of hollow to second stable site of top of DMPI cation with different time step. Here the brown, cyan, blue, magenta, and green colours represent the graphite carbon, DMPI cation's carbon, nitrogen, hydrogen and C2 carbon of DMPI cation, respectively.

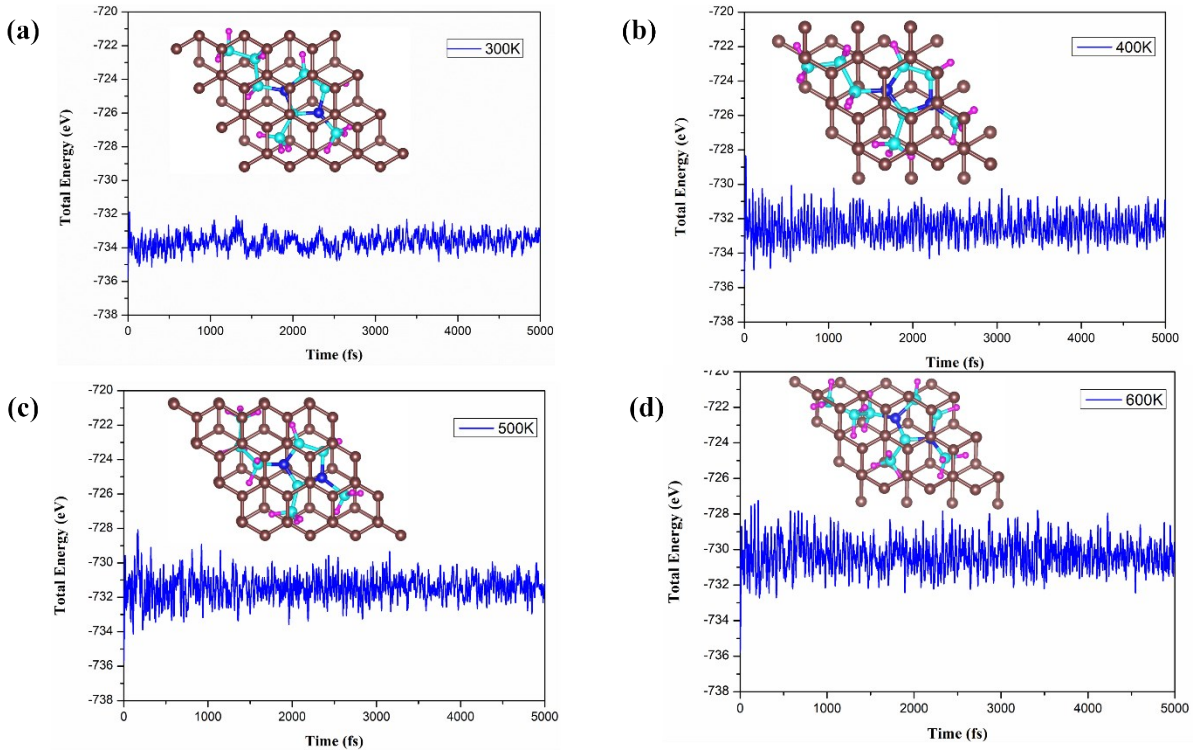

Figure S3. Schematic diagram of total energy from the molecular dynamics analysis at different temperatures as a function of time step and structure obtained, (a) 300 K, (b) 400 K, (c) 500 K and (d) 600 K.

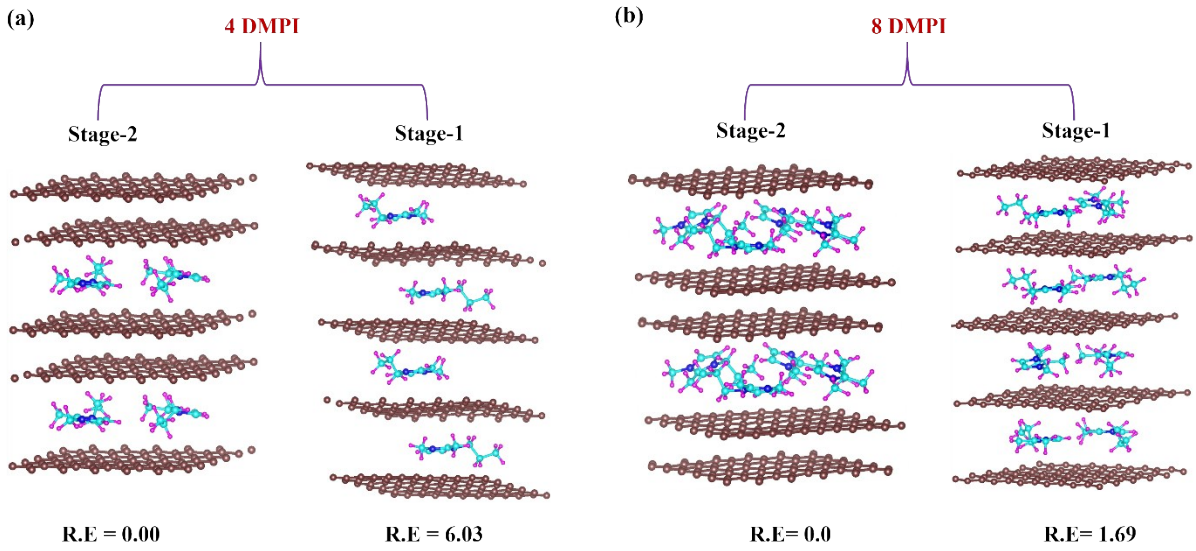

Figure S4. Comparative study of stage-1 and stage-2 DMPI intercalated graphite system for different concentration of the DMPI cation, (a) 4 DMPI and (b) 8 DMPI. Increase in DMPI concentration, stabilises the stage-1 DMPI intercalated graphite systems. R.E unit is eV.

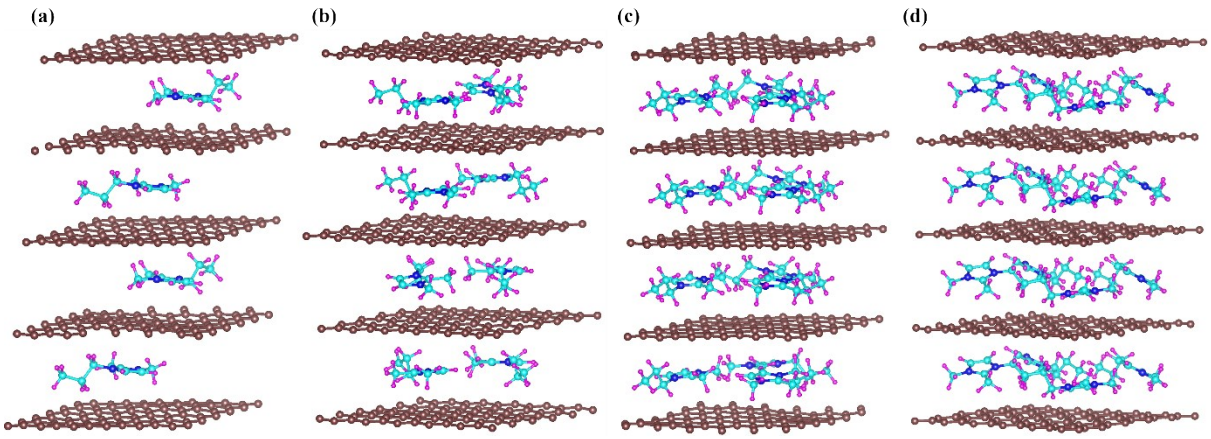

Figure S5. Pictorial representation of $6 \times 6 \times 2$ supercell of stage-1 DMPI intercalated graphite system with different DMPI cation concentration, (a) $C_{288}(DMPI)_4$, (b) $C_{288}(DMPI)_8$, (c) $C_{288}(DMPI)_{12}$ and (d) $C_{288}(DMPI)_{16}$.

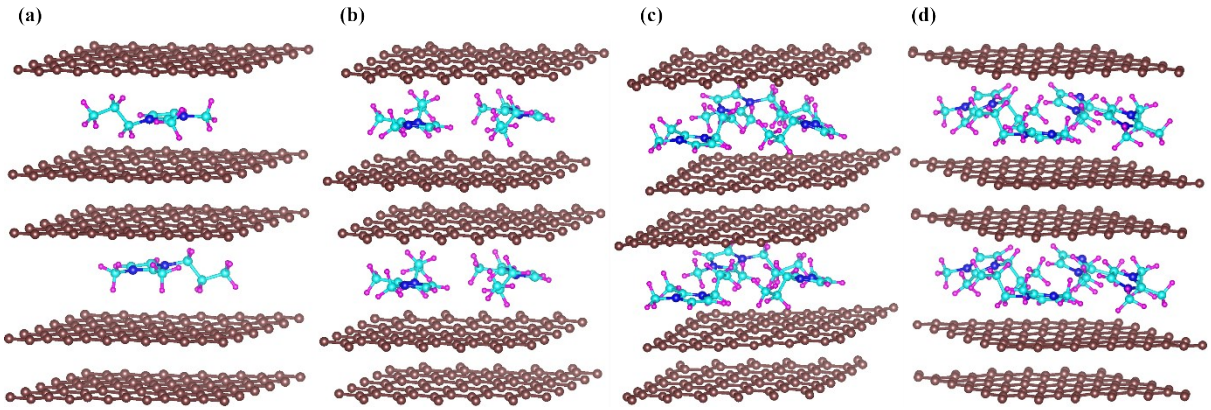

Figure S6. Pictorial representation of $6 \times 6 \times 2$ supercell of stage-2 DMPI intercalated graphite system with different DMPI cation concentration, (a) $C_{288}(DMPI)_2$, (b) $C_{288}(DMPI)_4$, (c) $C_{288}(DMPI)_6$ and (d) $C_{288}(DMPI)_8$.

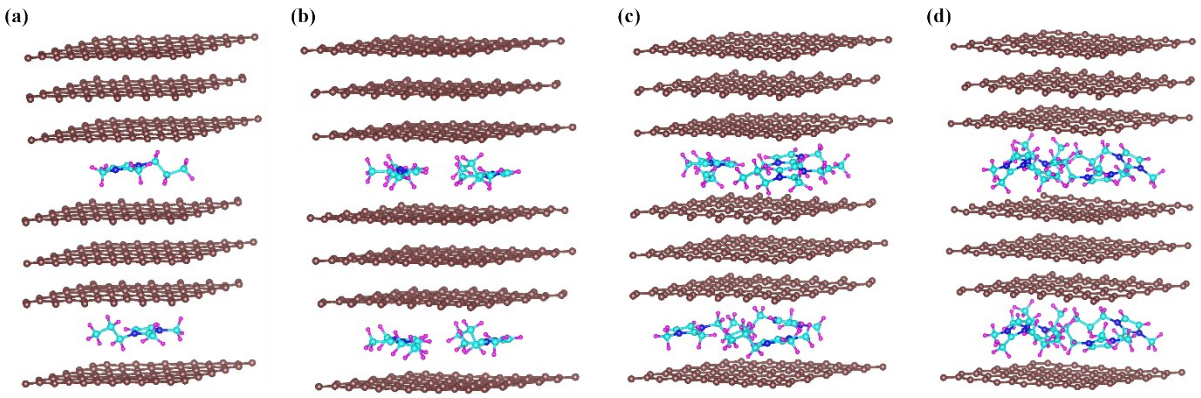

Figure S7. Pictorial representation of 6 × 6 × 3 supercell of stage-3 DMPI intercalated graphite system with different DMPI cation concentration, (a) $C_{432}(DMPI)_2$, (b) $C_{432}(DMPI)_4$, (c) $C_{432}(DMPI)_6$ and (d) $C_{432}(DMPI)_8$.

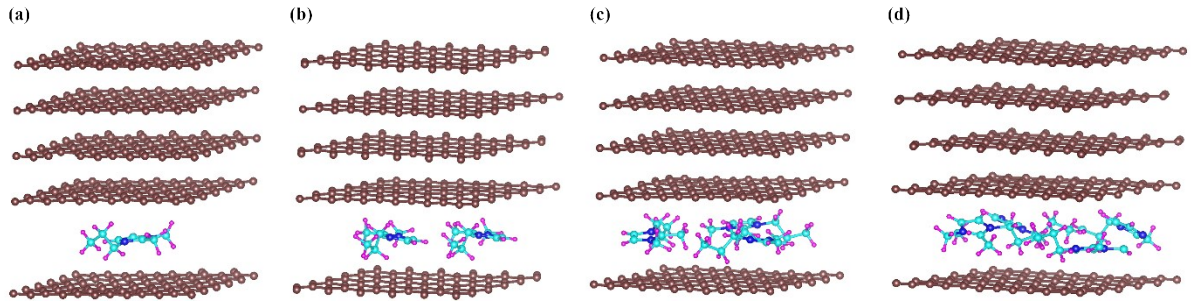

Figure S8. Pictorial representation of 6 × 6 × 2 supercell of stage-4 DMPI intercalated graphite system with different DMPI cation concentration, (a) $C_{288}(DMPI)_1$, (b) $C_{288}(DMPI)_2$, (c) $C_{288}(DMPI)_3$ and (d) $C_{288}(DMPI)_4$.

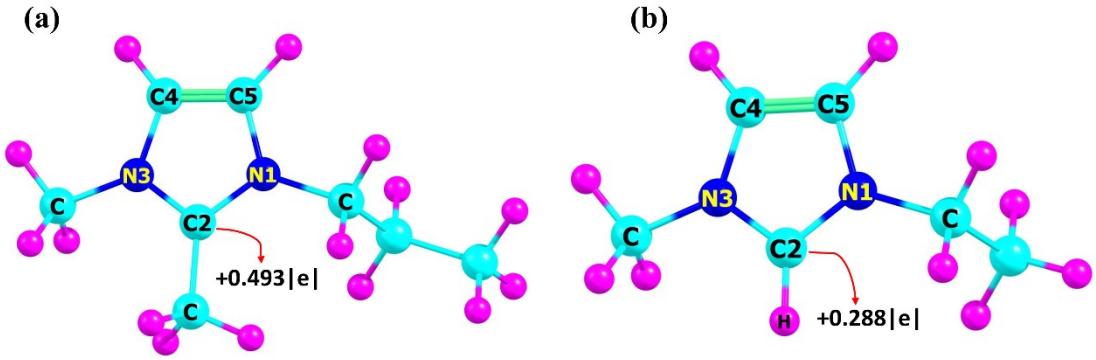

Figure S9. Schematic representation of NBO charge analysis on the C2 carbon atom of (a) DMPI and (b) EMI cations.

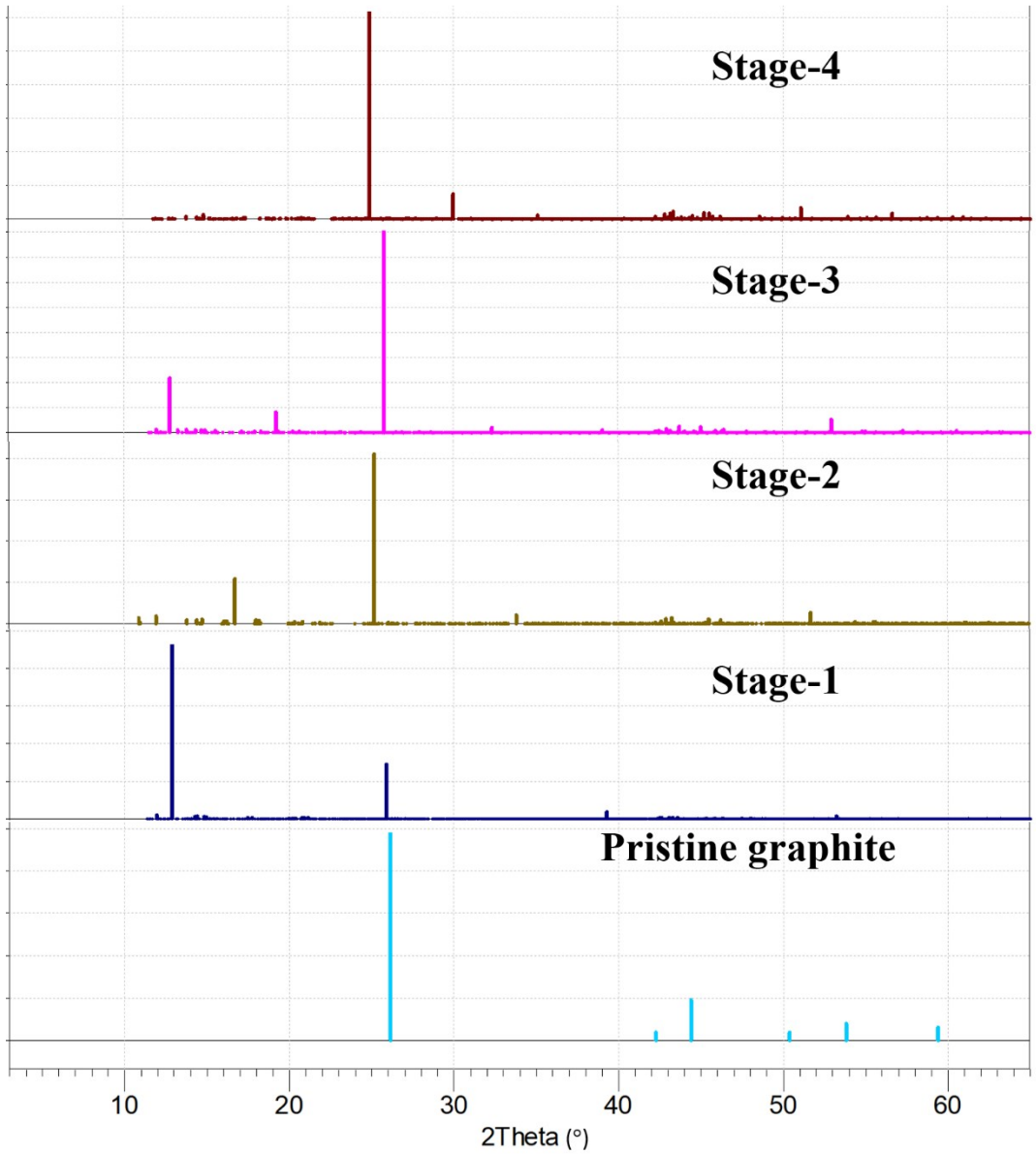

Figure S10. Simulated XRD pattern of the different staging of DMPI intercalated graphite system and pristine graphite where 2θ ranges in 3° – 65°.

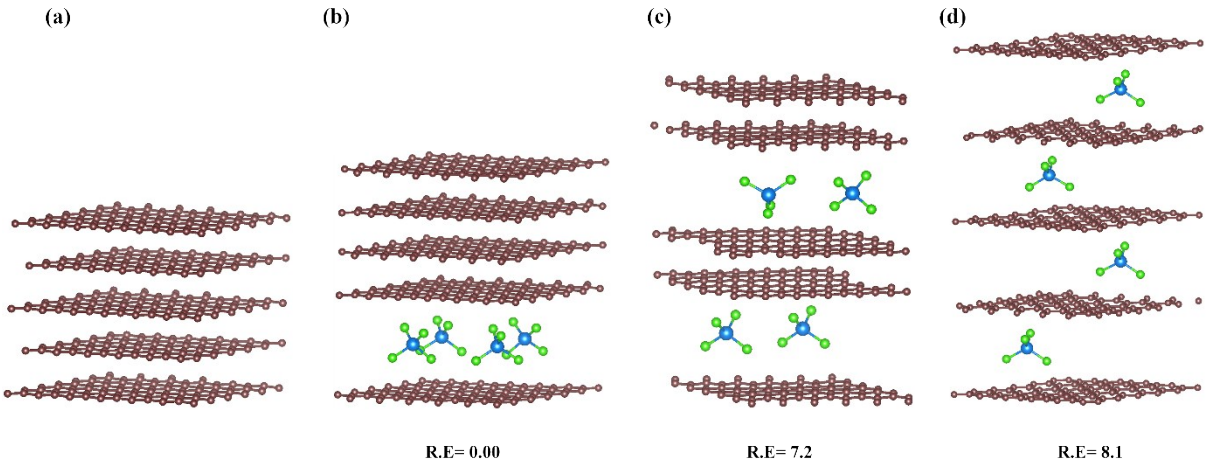

Figure S11. Systematic illustration of different staging mechanism of $AlCl_4$ anion intercalation, (a) graphite, (b) stage-4, (c) stage-2, and (d) stage-1, where R.E (eV) is the relative energies of same concentration of $AlCl_4$ ions. Here, brown, blue and green colour represents carbon, aluminium and chlorine, respectively.

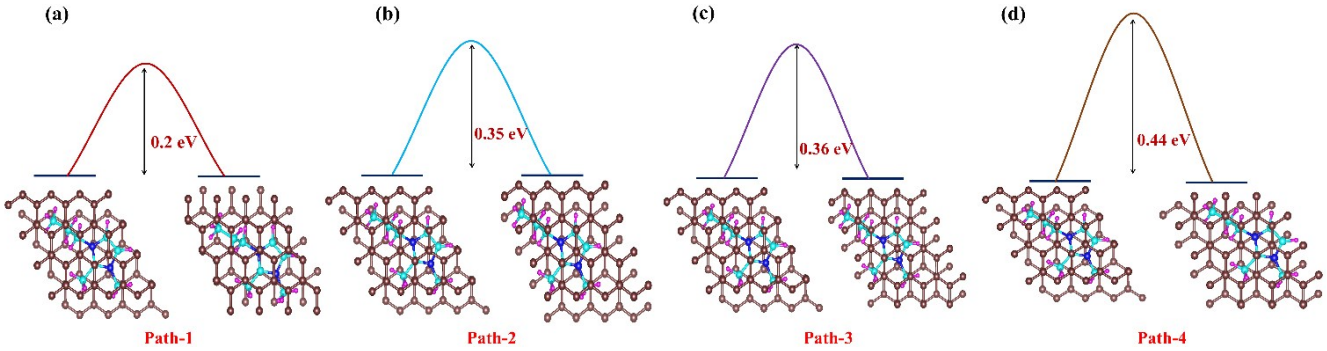

Figure S12. Schematic representation of the four diffusion barriers pathway, where (a-d) corresponds to path 1-4.